

**Production of medium-chain-length PHA in octanoate-fed enrichments dominated by *Sphaerotilus* sp.**

Vermeer, Chris M.; Depaz, Lena; van den Berg, Emily; Koelmans, Tom; Kleerebezem, Robbert

**DOI**

[10.1002/bit.28306](https://doi.org/10.1002/bit.28306)

**Publication date**

2022

**Document Version**

Final published version

**Published in**

Biotechnology and Bioengineering

**Citation (APA)**

Vermeer, C. M., Depaz, L., van den Berg, E., Koelmans, T., & Kleerebezem, R. (2022). Production of medium-chain-length PHA in octanoate-fed enrichments dominated by *Sphaerotilus* sp. *Biotechnology and Bioengineering*, 120(3), 687-701. <https://doi.org/10.1002/bit.28306>

**Important note**

To cite this publication, please use the final published version (if applicable). Please check the document version above.

**Copyright**

Other than for strictly personal use, it is not permitted to download, forward or distribute the text or part of it, without the consent of the author(s) and/or copyright holder(s), unless the work is under an open content license such as Creative Commons.

**Takedown policy**

Please contact us and provide details if you believe this document breaches copyrights. We will remove access to the work immediately and investigate your claim.

# eBook on Bioprocessing Basics


Bioreactors are more than just vessels! Do you want to learn more about the key characteristics of a bioreactor and the differences between batch, fed-batch, and continuous fermentation modes? Then download our eBook in which we provide information on the basics of bioprocessing.

Get your free copy now!

<https://eppendorf.group/bioprocessing-basics>



# Production of medium-chain-length PHA in octanoate-fed enrichments dominated by *Sphaerotilus* sp.

Chris M. Vermeer  | Lena Depaz | Emily van den Berg | Tom Koelmans | Robbert Kleerebezem

Department of Biotechnology, Delft University of Technology, Delft, The Netherlands

## Correspondence

Chris M. Vermeer, Department of Biotechnology, Delft University of Technology, Van der Maasweg 9, 2629 HZ Delft, The Netherlands.  
Email: [c.m.vermeer@tudelft.nl](mailto:c.m.vermeer@tudelft.nl)

## Funding information

Nederlandse Organisatie voor Wetenschappelijk Onderzoek

## Abstract

Medium-chain-length polyhydroxyalkanoate (mcl-PHA) production by using microbial enrichments is a promising but largely unexplored approach to obtain elastomeric biomaterials from secondary resources. In this study, several enrichment strategies were tested to select a community with a high mcl-PHA storage capacity when feeding octanoate. On the basis of analysis of the metabolic pathways, the hypothesis was formulated that mcl-PHA production is more favorable under oxygen-limited conditions than short-chain-length PHA (scl-PHA). This hypothesis was confirmed by bioreactor experiments showing that oxygen limitation during the PHA accumulation experiments resulted in a higher fraction of mcl-PHA over scl-PHA (i.e., a PHA content of 76 wt% with an mcl fraction of 0.79 with oxygen limitation, compared to a PHA content of 72 wt% with an mcl-fraction of 0.62 without oxygen limitation). Physicochemical analysis revealed that the extracted PHA could be separated efficiently into a hydroxybutyrate-rich fraction with a higher  $M_w$  and a hydroxyhexanoate/hydroxyoctanoate-rich fraction with a lower  $M_w$ . The ratio between the two fractions could be adjusted by changing the environmental conditions, such as oxygen availability and pH. Almost all enrichments were dominated by *Sphaerotilus* sp. This is the first scientific report that links this genus to mcl-PHA production, demonstrating that microbial enrichments can be a powerful tool to explore mcl-PHA biodiversity and to discover novel industrially relevant strains.

## KEYWORDS

medium-chain-length polyhydroxyalkanoates, microbial enrichment cultures, octanoate, poly(3-hydroxyhexanoate), poly(3-hydroxyoctanoate), *Sphaerotilus* sp

## 1 | INTRODUCTION

Polyhydroxyalkanoate (PHA) has attracted widespread attention as a biobased and biodegradable alternative to petrochemical-based materials. A broad range of bacteria is able to produce this biopolymer as an

intracellular storage compound (Steinbüchel, 1991). The type of PHA monomer produced is determined by the substrate provided, the environmental conditions, and the microorganism. In its turn, the type of PHA polymer will determine the physicochemical properties of the final product (Steinbüchel and Valentin, 1995; Zheng et al., 2020).

This is an open access article under the terms of the Creative Commons Attribution License, which permits use, distribution and reproduction in any medium, provided the original work is properly cited.

© 2022 The Authors. *Biotechnology and Bioengineering* published by Wiley Periodicals LLC.

PHA can potentially be produced cost-effectively by using microbial enrichments cultures and organic waste streams as feedstock. This approach diminishes the relatively large expenses for sterilization and raw substrates as required for pure culture production (Kleerebezem & van Loosdrecht, 2007), and avoids part of the waste disposal costs (Fernández-Dacosta et al., 2015). To date, at least 19 pilot studies have been conducted, using municipal or industrial organic waste streams as feedstock (Estévez-Alonso et al., 2021). In all these studies, the predominant type of PHA produced was the copolymer poly(3-hydroxybutyrate-co-3-hydroxyvalerate) (PHBV).

For thermoplastic applications, the mechanical properties of PHBV are already superior to the homopolymer, polyhydroxybutyrate (PHB) (Jain & Tiwari, 2015). However, incorporating medium-chain-length PHA (mcl-PHA) monomers in the polymer is required for elastomeric applications. Mcl-PHA consists of larger monomers ranging from 6 to 14 carbons, while short-chain-length PHA (scl-PHA) consists of monomers with 3–5 carbons. Increasing the mcl-PHA monomer composition in the polymer will result in a lower melting temperature, a lower degree of crystallinity, a lower tensile strength, and a higher elongation to break (Anjum et al., 2016; Rai et al., 2011). The production of these elastomers can expand the product utilization spectrum of PHA in the future, thereby potentially targeting rubber-like materials or adhesives (Elbahloul & Steinbüchel, 2009; Pereira et al., 2019).

The microbial metabolism to produce mcl-PHA is much less widespread than the metabolism for scl-PHA. In general, mcl-PHA production is linked to a special class of PHA synthases (PhaC Class II) possessed by a small number of organisms such as the well-studied *Pseudomonas* sp. or *Comamonas* sp. (Rai et al., 2011; Tortajada et al., 2013). However, some studies assert that in rare cases other classes of PHA synthases (Classes I and III) can incorporate hydroxyhexanoate (HHx) or hydroxyoctanoate (HO) monomers in the polymer (Quillaguamán et al., 2010; Sudesh et al., 2000). Because mcl-PHA metabolism appears to be sparse in the microbial world and because the available knowledge is incomplete, applying enrichment techniques offers an adequate approach to explore microbial diversity (Stouten, 2019).

The vast majority of the mcl-PHA research has been conducted with pure cultures. Nevertheless, a small number of laboratory studies focused on using microbial enrichments with feast–famine conditions. This intermittent substrate feeding strategy generates a competitive advantage for bacteria that store PHA as carbon and electron reservoir inside their cell. A proof-of-principle was already established with C8, C9, C12, and C18 fatty acids (Alaux et al., 2022; Chen et al., 2018; Lee et al., 2011; Shen et al., 2015), where it was found that medium-chain fatty acids form a suitable substrate for the enrichment of mcl-PHA producers. The mcl-PHA fractions of the total PHA content ranged from 0.06 to 0.88. However, the maximal obtained PHA contents were still rather low (23–49 wt%) compared to scl-PHA enrichment studies (Johnson, Jiang, et al., 2009; Kourmentza et al., 2017). In addition, an approach to understand and control the ratio between scl-PHA and mcl-PHA is still lacking.

PHA production from organic waste streams typically starts with the anaerobic fermentation of the feedstock where volatile fatty

acids (VFAs) are formed, ranging from acetate to hexanoate (Kleerebezem et al., 2015; Silva et al., 2022). Via a chain elongation step, the carbon chain of these VFAs can be extended to synthesize octanoate or more hexanoate (Angenent et al., 2016; Kucek et al., 2016). Although hexanoate is industrially more relevant than octanoate, in this research, octanoate was used as the sole carbon source because octanoate is regarded as a substrate that results in one of the highest mcl-PHA productivities (Li et al., 2021; Sun et al., 2007). Therefore, the aim of this research is to study which enrichment strategies result in a community with a high mcl-PHA storage capacity when feeding octanoate.

To this end, sequencing batch reactors (SBRs) were operated with synthetic octanoate as substrate in a mineral medium. Analysis of the PHA metabolic pathways revealed that the production of mcl-PHA requires less oxygen respiration than scl-PHA production. This resulted in the hypothesis that mcl-PHA production has a competitive advantage over scl-PHA production in an oxygen-limited environment. Therefore, the dissolved oxygen (DO) concentration was varied to understand and modify the enrichment process in terms of PHA content and composition. In addition, the pH of the SBRs was varied to study the effect of the toxicity of undissociated octanoic acid. For every operational steady state, the performance of the enrichments was characterized, including the maximum PHA storage capacity by means of accumulation experiments. An existing metabolic and kinetic model was adapted towards octanoate to derive the stoichiometric and kinetic parameters of all experiments (Johnson, Kleerebezem, et al., 2009). Finally, physicochemical polymer properties were determined to reveal information about the microbial origin of the produced polymer.

## 2 | MATERIALS and METHODS

### 2.1 | Enrichment in SBRs

Two double-jacket glass bioreactors with a working volume of 1.4 L (Applikon Biotechnology) were operated for the enrichment of a PHA-storing microbial culture on octanoate. The setup and operation of these bioreactors were based on the conditions described by Johnson, Jiang et al. (2009). The bioreactors were operated as nonsterile SBRs, subjected to a feast–famine regime with a cycle length of 12 h and solids retention time (SRT) and hydraulic retention time of 24 h, which implies that every cycle 50% of the SBR volume is replaced with fresh medium. The inoculum of the SBRs was aerobic-activated sludge of a wastewater treatment plant (WWTP) (Harnaschpolder Delfluent). Furthermore, the airflow rate to the bioreactors was set to 0.2 L<sub>N</sub>/min by means of a mass flow controller (MX4/4; DASGIP®), and the stirring speed was set to 800 rpm (TC4SC4; DASGIP®). The temperature in the bioreactor was controlled at 30 ± 0.5°C with the water jacket around the bioreactor and an external thermostat bath (ECO RE 630S). The pumps for feeding, effluent removal, and pH control, the stirrer, and the airflow were controlled by a hardware abstraction layer (TU Delft), which, in

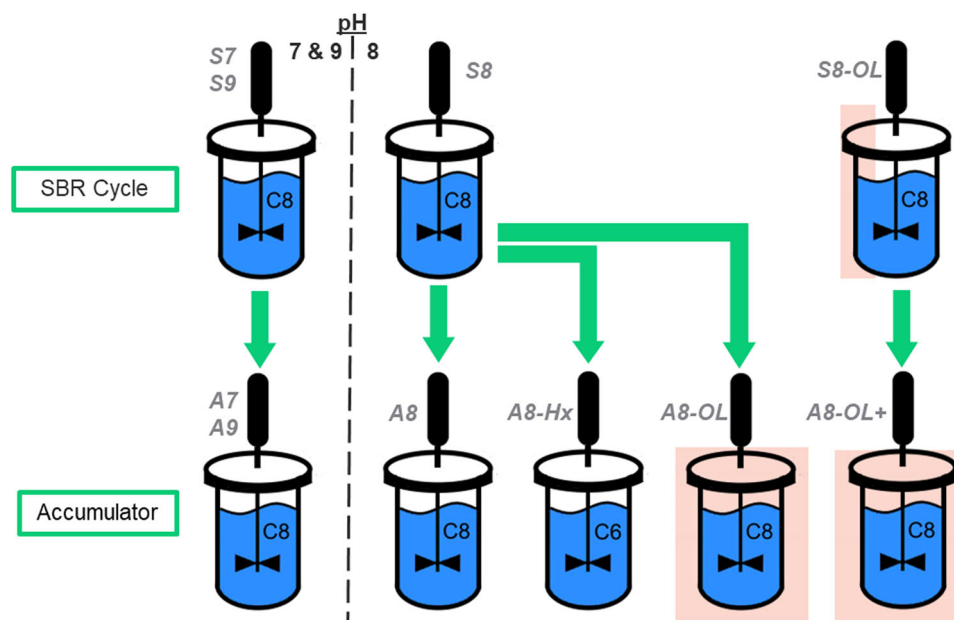


**FIGURE 1** Experimental overview of this study. C8 refers to octanoate and C6 refers to hexanoate as substrate. The name of each experiment is displayed in grey. Experiments under oxygen limitation (OL) are indicated by the pink areas. SBR, sequencing batch reactors.

turn, was controlled by a PC using a custom scheduling software (D2I; TU Delft). The D2I was also used for data acquisition of the online measurements: DO, pH, temperature, acid and base dosage, in- and off-gas composition, and feed/water balances. The addition of nutrients and carbon sources at the beginning of each cycle was followed by a phase of a high oxygen uptake rate, of which the duration and the magnitude were extracted from the off-gas data. Moreover, the bioreactors were cleaned about twice per week to remove biofilms from the glass walls and the sensors of the bioreactor. The medium consisted of a separate carbon and nutrient source. The carbon source concentration in the SBR was 4.75 mM octanoate. The nutrients concentrations in the SBR were composed of 6.74 mM  $\text{NH}_4\text{Cl}$ , 2.49 mM  $\text{KH}_2\text{PO}_4$ , 0.55 mM  $\text{MgSO}_4 \cdot \text{H}_2\text{O}$ , 0.72 mM KCl, 1.5 ml/L trace elements solution according to Vishniac and Santer (1957), and 5 mg/L allylthiourea (to prevent nitrification). To characterize the operational performances, the SBRs were subjected to multiple cycle analysis experiments.

## 2.2 | PHA accumulation in fed-batch bioreactor

The PHA accumulation experiments were performed in the same bioreactors as the enrichment but operated in fed-batch mode. The pH, temperature, and aeration rate were copied from the corresponding SBR. Half of the content of the SBR (700 ml) of the final cycle was used as seeding material for the accumulation experiment. In addition, 700 ml medium was supplied as described above, but without ammonium and carbon source. After 30 min, to ensure a temperature of 30°C, a pulse of 6.7 mmol octanoates was supplied to each bioreactor. To prevent carbon source depletion

throughout the PHA accumulation, octanoic acid (undiluted) and NaOH (1 M) were used to control the pH. In addition, pulses of 0.67 mmol octanoates were supplied every 2 h from  $t = 4$  h to the end of the experiment. One accumulation was performed by replacing octanoate and octanoic acid with hexanoate and hexanoic acid. Nitrogen was limited during most of the accumulation since no nitrogen source was supplied to the bioreactors and only a small amount ( $<1.7$  mM of  $\text{NH}_4^+$ ) remained from the previous SBR cycle. In this way, growth in the fed-batch bioreactor was limited. If necessary, a few drops of (10X diluted) Antifoam C (Sigma-Aldrich) were added to inhibit the formation of foam. The experiments were terminated after 24 h.

## 2.3 | Varying pH in the bioreactor

The pH was maintained by the addition of 1 M HCl and 1 M NaOH through an integrated revolution counter (MP8, DASGIP®; Eppendorf). During the first enrichment (S7), the set point of the SBR and the accumulation bioreactor were  $7.0 \pm 0.1$ . The set point was increased to  $8.0 \pm 0.1$  and  $9.0 \pm 0.1$  in the second (S8) and third enrichment (S9), respectively, and the corresponding accumulations (A8 and A9) (Figure 1). The microbial community of the first enrichment was used as inoculum for the second enrichment, and the microbial community of the second enrichment was used as inoculum for the third enrichment. In addition, every new enrichment was supplemented with fresh aerobic-activated sludge from the WWTP. The oxygen transfer limitation experiments (Section 2.4) and hexanoate accumulation were conducted at  $\text{pH } 8.0 \pm 0.1$ . All different operational states in this study were enriched for at least 70 cycles.

## 2.4 | DO limitation

In aerobic feast–famine SBRs, oxygen consumption is a key indicator of the PHA production behavior of the community (Stouten, Hogendoorn, et al., 2019). The fraction of the cumulative amount of oxygen consumed in the feast phase ( $O_{2, \text{feast}}$ ) was calculated several SBR cycles by using

$$O_{2, \text{feast}} (\%) = \frac{\text{Cum. } O_{2, \text{feast}} (\text{mol})}{\text{Cum. } O_{2, \text{feast}} (\text{mol}) + \text{Cum. } O_{2, \text{famine}} (\text{mol})} \quad (1)$$

Moreover, the influence of the DO concentration, and the corresponding oxygen consumption rate, on the PHA composition was investigated. DO limitation was achieved by lowering the stirrer speed from 800 to 200 rpm when the substrate was available. This means that during the enrichment the stirrer speed was automatically lowered during the feast phase (S8-OL Figure 1). For both enrichment S8 and S8-OL, an oxygen-limited accumulation experiment was conducted to test the maximum PHA storage capacity (A8-OL and A8-OL+, respectively). During the oxygen-limited accumulation experiments, the stirrer speed was at all times 200 rpm. The microbial community of the enrichment at pH 8 was used as starting material for the oxygen-limited enrichment, again supplemented with fresh aerobic-activated sludge from the WWTP. The volumetric mass transfer coefficient ( $k_L a$ ) for a stirrer speed of 200 and 800 rpm was determined by using the dynamic gassing out method (Garcia-Ochoa & Gomez, 2009; Van't Riet, 1979) under the operational conditions of the experiment.

## 2.5 | PHA extraction and fractionation

During the accumulation experiments, 50 ml cell suspension was collected from the bioreactor after 12 h. After centrifuging and freeze-drying,  $\pm 350$  mg of the dried biomass was mixed with 12.5 ml chloroform. The suspension was incubated for 3 h at 60°C while manually shaken every 30 min. Then, the suspension was filtered (0.45  $\mu\text{m}$  filter). Lastly, the chloroform was evaporated in a fume hood to obtain purified PHA.

Part of the purified PHA from the accumulation at pH 8 (A8) was fractionated by selective precipitation. To this end, the PHA was divided into five parts of  $\pm 20$  mg and redissolved in 0.8 ml chloroform. Different volumes of antisolvent (1-heptane) were added (0.9, 1.1, 1.4, 1.6, and 15). After 15 min incubation, the tubes were centrifuged and the supernatant was decanted into another tube. Only the tube with 15 volumes of 1-heptane was incubated for 48 h. Then, the solvent–antisolvent mixture in all tubes was evaporated in a fume hood. The obtained PHA fractions were analyzed by gas chromatography (GC).

## 2.6 | Analytical methods

The performance of the cycle and accumulation experiments were characterized by online measurements (DO, pH, acid/base dosage,

and in-/off-gas composition) with the equipment and software described above, and with offline samples (VFAs, ammonium, PHA, and total and volatile suspended solids). The composition of the active biomass was assumed to be  $\text{CH}_{1.8}\text{O}_{0.5}\text{N}_{0.2}$  (Beun et al., 2002). A detailed description of the analytical methods is given by Johnson, Jiang et al. (2009). A modification has been made to the ammonium measurement. These samples were measured with a Gallery™ Plus Discrete Analyzer (Thermo-Fisher Scientific).

The method to analyze the PHA composition of the biomass by GC was also modified to include mcl-PHA. In brief, the PHA in the biomass was hydrolyzed and esterified in the presence of concentrated acid, propanol, and dichloroethane with a ratio of 1/4/5 (vol/vol/vol) for 3 h at 100°C. In this research,  $\text{H}_2\text{SO}_4$  was used as acid instead of HCl. The formed propylesters, which accumulated in the organic phase, were analyzed by a GC (model 6890N; Agilent). The PHA analysis method was expanded to include the quantification of poly(3-hydroxyhexanoate) (PHHx) and poly(3-hydroxyoctanoate) (PHO) by using methyl 3-hydroxyhexanoate (Sigma-Aldrich) and methyl 3-hydroxyoctanoate (Santa Cruz Biotechnology) as standard.

GC–mass spectrometry (MS) analysis was carried out on a 7890A GC coupled to a 5975C quadrupole mass selective detector (both from Agilent) to identify PHB, PHHx, and PHO. Samples were pretreated in the same way as described for GC analysis. However, methanol was added instead of propanol to form methylesters. The mass spectrum of these methylesters was processed by the Mass Hunter Quantitative Analysis Software for compound identification. A detailed description of the analytical protocol is described by Velasco Alvarez et al. (2017).

Furthermore, the method for measuring volatile suspended solids was substituted by a thermogravimetric analysis (TGA) using a Perkin Elmer TGA 8000. Around 2 mg of freeze-dried biomass, the sample was heated from 35°C to 105°C (10°C/min), followed by an isothermal step (100 min), followed by second heating run from 105°C to 550°C (10°C/min), followed by a second isothermal step (60 min). All steps were under a nitrogen atmosphere, while in the last isothermal step, the nitrogen gas was switched to air. The TGA data was also applied as an alternative method to determine the PHA weight percentage of the biomass (Chan et al., 2017).

A differential scanning calorimeter (DSC) measurement was performed to measure the melting ( $T_m$ ) temperature of the extracted PHA (Section 2.4) using a Perkin Elmer DSC-7. First, the PHA sample was cooled from 25 to  $-70^\circ\text{C}$  at a rate of 20°C/min. Then, the PHA sample was heated from  $-70^\circ\text{C}$  to 180°C at the same rate. After 10 min at 180°C, the sample was quench cooled to  $-70^\circ\text{C}$  at a rate of 100°C/min. In a second heating run, the sample was heated again to 140°C at a rate of 20°C/min. This run was used for  $T_m$  determination. All steps were performed under a nitrogen atmosphere. A poly(3-hydroxybutyrate-co-3-hydroxyvalerate-co-3-hydroxyhexanoate) (PHBVHx) (94%/2%/4%) reference sample (Sigma-Aldrich) was measured for comparative purposes.

A gel permeation chromatography (GPC) measurement was performed to measure the molecular weight distribution of the extracted PHA (Section 2.4) using a Shimadzu Prominence GPC

system equipped with a Shodex LF-804 column. Dimethyl furan (DMF) was used as the eluent at a flow rate of 1 ml/min at 40°C. Before injection, the PHA sample was first dissolved in chloroform at a concentration of 30 mg/ml, then diluted with nine volumes of DMF, and subsequently filtered. Data from the refractive index detector was quantified with a universal calibration of monodisperse polystyrene standards with the help of LabSolutions software.

## 2.7 | Microbial community analysis

To analyze the microbial composition of the enriched cultures, 2 ml of bioreactor content was collected in an Eppendorf tube. These samples were taken approximately two times per week during the enrichment phase and in addition during the cycle and accumulation experiments. The tubes were centrifuged (13,300g; 5 min). The pellet was stored at -20°C until analysis. After defrosting, genomic DNA was extracted using the DNeasy UltraClean Microbial Kit (Qiagen), following the manufacturer's instructions. DNA quantification was carried out using the Qubit® dsDNA Broad Range Assay Kit (Qubit® 2.0 Fluorometer; Thermo Fisher Scientific), following the manufacturer's instructions. Afterward, about 50 µl of isolated (16S) DNA was sent to Novogene Ltd. for amplicon sequencing of the V3-4 region of the 16S ribosomal RNA gene and for metagenomic sequencing. A description of the procedure for metagenomic sequencing is presented by Pabst et al. (2021). Various genomic fragments were aligned with published sequences from GenBank using the NCBI BLAST tool to find related genes and strains (Altschul et al., 1990). All sequence data of this study have been deposited in GenBank with BioProject ID PRJNA831682.

## 2.8 | Metabolic model and parameter identification

A metabolic and kinetic model proposed by Johnson, Kleerebezem et al. (2009) was used as starting point for this study. The previous model was transformed from acetate uptake and PHB production to octanoate (and hexanoate) uptake and PHB, PHHx, and PHO production (Supporting Information: Figure S1 and Table S1). The model contains a set of metabolic and kinetic expressions which together describe the consumption and formation of the main compounds in the bioreactor, that is PHA (PHB, PHHx, and PHO), biomass, organic substrate, CO<sub>2</sub>, O<sub>2</sub>, and ammonium.

The obtained reactions were used to calculate the stoichiometric yields by balancing the conserved moieties (octanoyl-CoA, hexanoyl-CoA, butyryl-CoA, acetyl-CoA, NADH, ATP). The stoichiometric yields and the kinetic expressions shown in Supporting Information: Tables S2 and S3 form the basis of the model. The stoichiometric yields that encompassed PHA were calculated by multiplying the stoichiometric yield of the specific PHA type by the fraction of this type of PHA at the moment the cellular PHA content was maximal, as shown in the example of PHA yield on the substrate ( $Y_{PHA,S}$  in Cmol/Cmol) in

$$Y_{PHA,S} = Y_{PHB,S} \cdot \frac{PHB_{max}}{PHA_{max}} + Y_{PHHx,S} \cdot \frac{PHHx_{max}}{PHA_{max}} + Y_{PHO,S} \cdot \frac{PHO_{max}}{PHA_{max}} \quad (2)$$

Here,  $Y_{PHB/PHHx/PHO,S}$  (Cmol/Cmol) describe the stoichiometric yield of the specific type of PHA on the substrate, and  $\frac{PHB/PHHx/PHO_{max}(Cmol)}{PHA_{max}(Cmol)}$  describe the fraction of this type of PHA measured by GC analysis.

The trends obtained by the model are fitted to the experimental data. Then, the biomass-specific rates and actual yields were derived from the model. Throughout this work, PHO, PHHx, or PHB are defined as monomers of HO, HHx, or hydroxybutyrate (HB) embedded in a polymer, respectively, regardless of whether this is a copolymer or a homopolymer.

## 3 | RESULTS

### 3.1 | Start enrichment

As the experiment at pH 7 proceeded, both the duration of the feast phase (feast time) and the fraction of oxygen consumed in the feast phase ( $O_{2,feast}$ , as calculated by Equation 1) showed a downward trend (Figure 2a). The shift in both variables suggested that the community shifted from a growth-oriented strategy towards a PHA hoarding strategy. The PHA analysis data confirmed this hypothesis by revealing that PHA production in the form of PHB was low in the first cycles but significantly increased between the 10th and 24th cycles (Figure 2b). Then, the first stable phase commenced (Cycles 22–38) which was characterized by PHB production (42 wt% at the end of the feast phase), an average feast time of  $81 \pm 18$  min, and an average  $O_{2,feast}$  of  $59 \pm 3\%$ . The amplicon sequencing data revealed that *Acinetobacter* sp. or *Zoogloea* sp. are likely to be responsible for this functionality (Figure 2c).

After the 38th cycle, another shift in functionality and community structure occurred followed by a second stable phase (Cycles 48–80). This phase is characterized by the production of PHA (42 wt%) consisting of HO (23 wt%), HHx (9 wt%), but also HB (10 wt%) monomers. This phase revealed a significantly lower average value for the  $O_{2,feast}$  ( $34 \pm 3\%$ ) compared to the first stable phase ( $59 \pm 3\%$ ). In addition, the feast times also showed a slight decrease ( $65 \pm 11$  min). A clear link with the 16S amplicon sequencing data is observed where *Sphaerotilus* sp. became abundant from the 38th cycle onwards and remained the dominant genus during the second stable phase (Figure 2). The identification of HB, HHx, and HO monomers in the polymer was confirmed by the characterization of the mass spectra after GC-MS analysis (data not shown).

### 3.2 | Performance of enrichment at varying pH

The pH of the bioreactor was increased from pH 7 to pH 8 and pH 9 in two consecutive enrichment experiments. At each pH, detailed

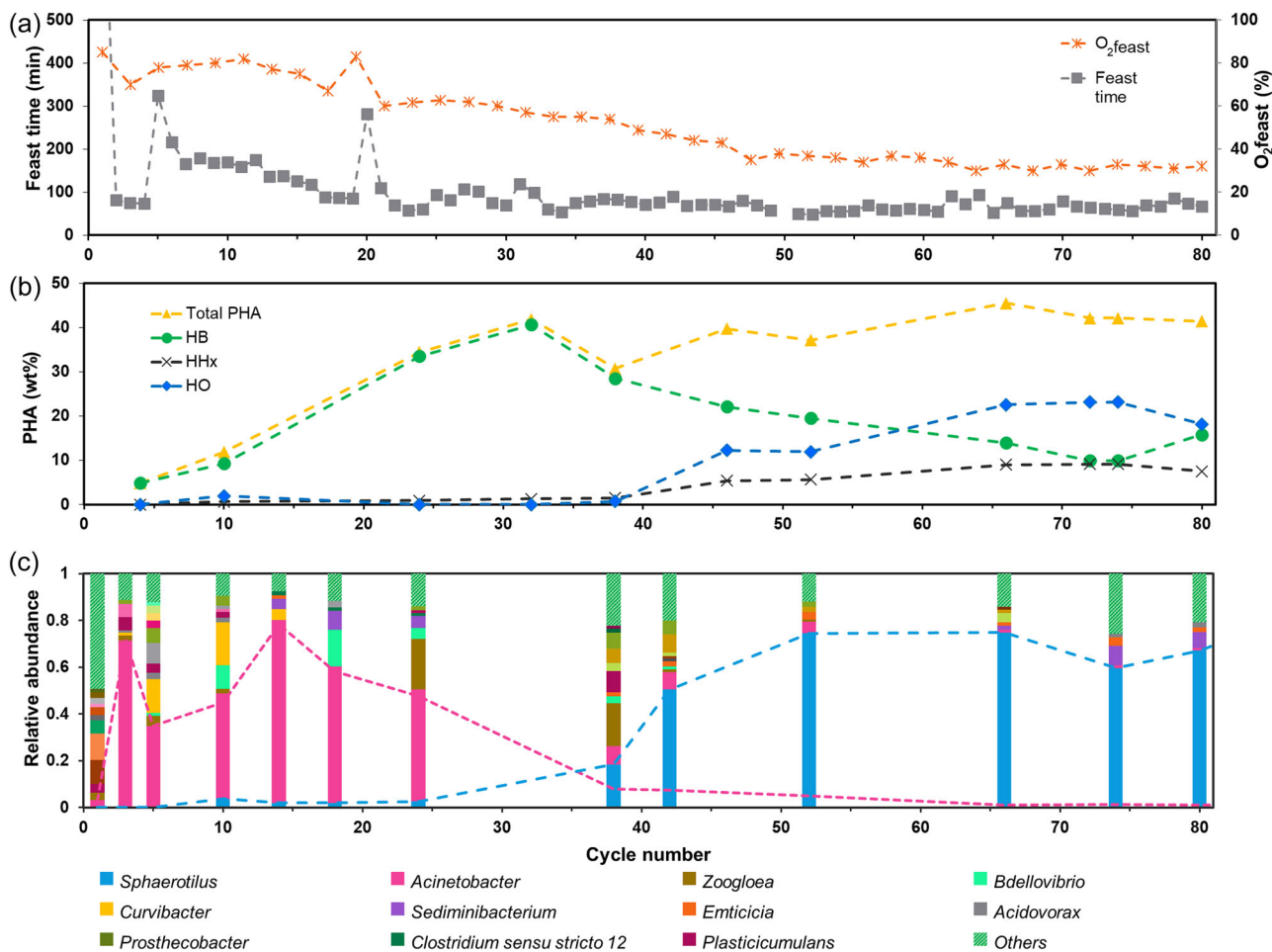


**FIGURE 2** Overview of online and offline data of the enrichment at pH 7. (a) The length of the feast phase (feast time) and the fraction of O<sub>2</sub> consumed in the feast phase (O<sub>2</sub>feast) are both derived from the off-gas data. (b) The PHA content at the end of the feast phase, including the specification of the different monomers. (c) The relative abundance of genera derived from 16S amplicon sequencing. The two most abundant genera are shown both with stacked columns and lines. Only genera with a relative abundance of more than 1% are depicted in the graph. HB, hydroxybutyrate; HHx, hydroxyhexanoate; HO, hydroxyoctanoate; PHA, polyhydroxyalkanoate.

insight into the performance of the enrichment was obtained by the analysis of an SBR cycle and an accumulation experiment. The main experimental results are presented in Figures 3 and 5a,c (pH = 8). More detailed information can be found in Table 1, and Supporting Information Online Materials: Figure S2 and Table S4.

The PHA content at the end of the feast phase appeared to be slightly higher for the enrichment at pH 8 (S8), than for the enrichment at pH 7 (S7) and pH 9 (S9). The PHA monomer composition was reasonably similar in S7 and S8, while in S9, more PHB was produced. For the maximum PHA content in the accumulation experiments, a similar trend was observed. The accumulation at pH 8 (A8) obtained the highest PHA content with 72 wt% PHA (HO fraction of 0.49, HHx fraction of 0.14, and HB fraction of 0.38). The biomass-specific PHA production rate ( $q_{\text{PHA, max}}$ ) remained fairly constant regardless of pH value. Interestingly, *Sphaerotilus* sp. was dominant at pH 7 and pH 8, while it was outcompeted at pH 9 as revealed by both 16S amplicon data and microscopic observations (data not shown). It was decided to

continue the following experiments at pH 8, as the results at pH 8 appeared to be most favorable in terms of PHA production. Nevertheless, it must be noted that the community at pH 8 was enriched for more cycles than the community in S7.

### 3.3 | The impact of oxygen limitation

The oxygen supply rate was decreased in the bioreactor to test the hypothesis that oxygen limitation favors the production of mcl-PHA over scl-PHA. This was achieved by lowering the stirrer speed during the feast phase of the SBR and during the whole accumulation. This resulted in a decrease of the  $k_L a$  from 93.5 to 5.3 h<sup>-1</sup> and a decrease in DO concentration from 5.7 mg/L to below 0.1 mg/L.

A significant increase in feast time was observed in the SBR with oxygen limitation (S8-OL) compared to the standard SBR (S8) (1.7 h instead of 1 h), indicating that the biomass-specific rates are impacted by the oxygen-limited environment (Figure 4 and Table 1). Aside from



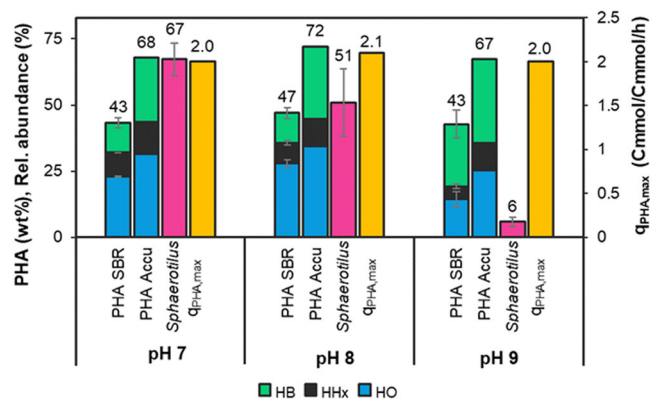


**FIGURE 3** Main results of the enrichment experiments at varying pH. “PHA SBR” is the average PHA wt% at the end of the feast phase over the last three samples of the SBR enrichment. “PHA Accu.” is the PHA wt% of the maximal value in the accumulation experiment. “Sphaerotilus” is the relative abundance of this genus in the 16S amplicon data over the last three samples of the enrichment.  $q_{\text{PHA,max}}$  is calculated from the SBR cycle analysis in the enrichment. In Supporting Information: Figure S2, all experimental results fitted with the metabolic model are shown, including off-gas, ammonium, and biomass. HB, hydroxybutyrate; HHx, hydroxyhexanoate; HO, hydroxyoctanoate; PHA, polyhydroxyalkanoate; SBR, sequencing batch reactors.

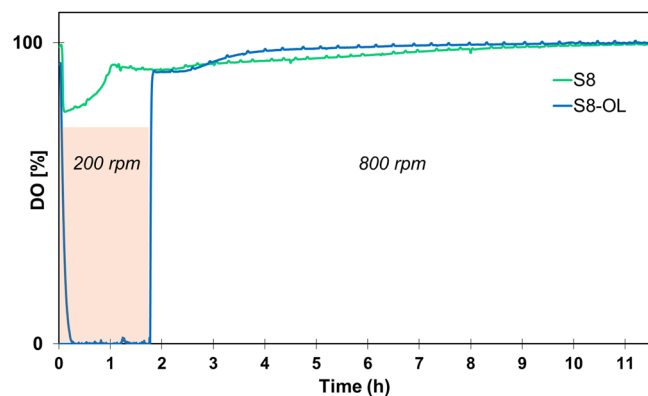


**FIGURE 4** Dissolved oxygen (DO) profile during one cycle of the standard sequencing batch reactors (SBRs) at pH 8 (S8) and of the SBR under oxygen limitation (S8-OL). For S8-OL, the stirrer speed is lowered to 200 rpm in the feast phase indicated by the pink area.

the difference in feast time, the PHA trends of the two-cycle analyses showed a similar profile (Figure 5a,b). No significant difference in the ratio of PHA monomers produced was observed. However, a slightly larger fraction of the substrate is directed towards PHA production under oxygen limitation indicated by a higher  $Y_{\text{PHA,S}}$ , and resulting in a higher PHA content at the end of the cycle in S8-OL (55 wt%) compared to S8 (46 wt%). Interestingly, the oxygen-limited regime did not cause a major shift in the microbial community structure; *Sphaerotilus* sp. remained the dominant genus.

Two accumulation experiments were performed under oxygen-limited conditions. A8-OL was inoculated with biomass from the SBR

at pH 8 without oxygen limitation (S8). A8-OL+ was inoculated from the oxygen-limited SBR (S8-OL) (see experimental overview in Figure 1). The results were compared to the standard accumulation at pH 8 (A8) (Figure 5c–e and Table 1). Although all biomass-specific rates decreased when oxygen limitation was imposed, the total amount of PHA after 12 h accumulation and the final PHA content was remarkably identical to nonoxygen-limited conditions (all experiments between 81.4 and 82.2 mCmol and between 71.9 and 76.5 wt%, respectively). Again, the yield values expressed that PHA production is slightly more efficient, and growth is slightly less efficient when oxygen is limited. A significant difference was detected in PHA composition when comparing the oxygen-limited accumulations (A8-OL and A8-OL+) to the standard accumulations (A8). The PHB content decreased significantly, the PHHx content remained fairly constant, and the PHO content increased significantly. Oxygen-limited conditions resulted in a higher mcl-fraction of the PHA, from 0.62 in A8 to 0.79 in A8-OL and 0.76 in A8-OL+. The difference between the two oxygen-limited accumulations (A8-OL and A8-OL+) is small in every aspect suggesting that the influence of enriching under oxygen limitation is minimal as was already expected from the analysis of the SBRs.

### 3.4 | Accumulation with hexanoate

One accumulation experiment was performed with hexanoate (A8-Hx) as the sole carbon source inoculated with biomass enriched on octanoate (S8) to see if high mcl-PHA contents could be produced from a substrate that is more relevant from an industrial perspective. Figure 5f reveals that the biomass demonstrated an instant response toward this new substrate. However, the biomass-specific rates as well as the final PHA amount and content were lower than in the standard accumulation (A8) (Table 1). Moreover, the PHA consisted predominantly of PHB while PHO was absent. The PHHx content was again very similar to A8.

### 3.5 | Bioreactor data validation

The carbon and electron balances of the SBR cycles closed on average for  $99.9 \pm 5.3\%$ . For the accumulation experiments, a gap in the mass balance developed over time, resulting in an average closure of  $66.5 \pm 13\%$ . Although these gaps have been observed in accumulation experiments of previous research (Marang et al., 2016; Vermeer et al., 2022), the gaps in this study are larger. A possible explanation for the large size of these gaps forms the feeding method during the accumulation which entails the addition of undiluted octanoic or hexanoic acid. It was hypothesized that the undiluted acid was not able to dissolve completely in the medium. To confirm this hypothesis, undiluted octanoic acid was fed to a bioreactor without biomass to aim for a concentration of 500 mg/L. Nevertheless, measurements showed that the medium contained  $420 \pm 6$  mg/L after 2 h of incubation with a stirrer speed

**TABLE 1** Overview of the main measured data, microbial community data (16S amplicon sequencing), and model-derived yields and biomass-specific rates of the cycle and accumulation experiments

	Unit	SBR cycles					Accumulations				
		S7	S8	S9	S8-OL	A7	A8	A9	A8-OL	A8-OL+	A8-Hx
Number of cycles enriched		80	99	70	70	80	89	70	93	70	99
Length feast phase	h	1.1	1.0	1.2	1.7	5.3	1.5	1.1	1.8	2.6	1.9
Total PHA max.	%	42	46	49	54	68	72	67	73	76	57
HB max.	%	10	12	24	14	24	27	32	18	16	49
HHx max.	%	9	7	7	9	12	10	10	10	11	8
HO max.	%	23	26	18	31	32	35	25	45	49	0
TGA	%	51.0	52	53	55	70	77	68	74	73	61
mcl-fraction		0.76	0.73	0.51	0.73	0.64	0.62	0.53	0.76	0.79	0.15
Fraction O <sub>2</sub> feast/O <sub>2</sub> consumed total (mmol)		0.28	0.33	0.27	0.26	55.4	39.3	40.5	32.3	27.8	39.1
<i>Sphaerotilus natans</i>		60%	43%	3%	77%	72%	43%	3%	64%	77%	70%
Other most abundant		Thau (39%)					Thau (39%)				
Second most abundant		Sedim (8%)					Phrea (20%)				
$\mu_{s,max}$	mCmol/mCmol/h	-2.30	-2.10	-2.00	-2.30	-0.70	-1.40	-1.4	-1.00	-0.8	-1.10
$\mu_{max}$	mCmol/mCmol/h	0.40	0.22	0.07	0.10	0.10	0.30	0.20	0.15	0.15	0.11
$\mu_{PHA,max}$	mCmol/mCmol/h	2.00	2.10	2.00	2.30	0.80	1.30	1.30	0.90	0.67	0.90
$Y_{X,S}$	mCmol/mCmol	0.19	0.11	0.04	0.05	0.15	0.20	0.22	0.16	0.13	0.13
$Y_{PHA,S}$	mCmol/mCmol	0.77	0.88	0.96	0.94	0.75	0.70	0.72	0.76	0.77	0.74
$Y_{O_2,PHA}$	mmol/mCmol	0.19	0.19	0.14	0.16	0.40	0.43	0.39	0.34	0.34	0.47
$Y_{O_2,S}$	mmol/mCmol	0.21	0.16	0.13	0.15	0.30	0.30	0.28	0.26	0.26	0.35

Abbreviations: A8-OL, oxygen-limited accumulation; Dechlo, *Dechloromonas* sp.; Ferru, *Ferruginibacter* sp.; HB, hydroxybutyrate; HO, hydroxyoctanoate; Leadb, *Leadbetterella* sp. mcl, medium chain length; PHA, polyhydroxyalkanoate; Phre, *Phreatobacter* sp.; S8-OL, SBR under oxygen limitation; SBR, sequencing batch reactors; Sedim, *Sediminibacter* sp.; TGA, thermogravimetric analysis; Thau, *Thauera* sp.; Zoo, *Zoogloea* sp.

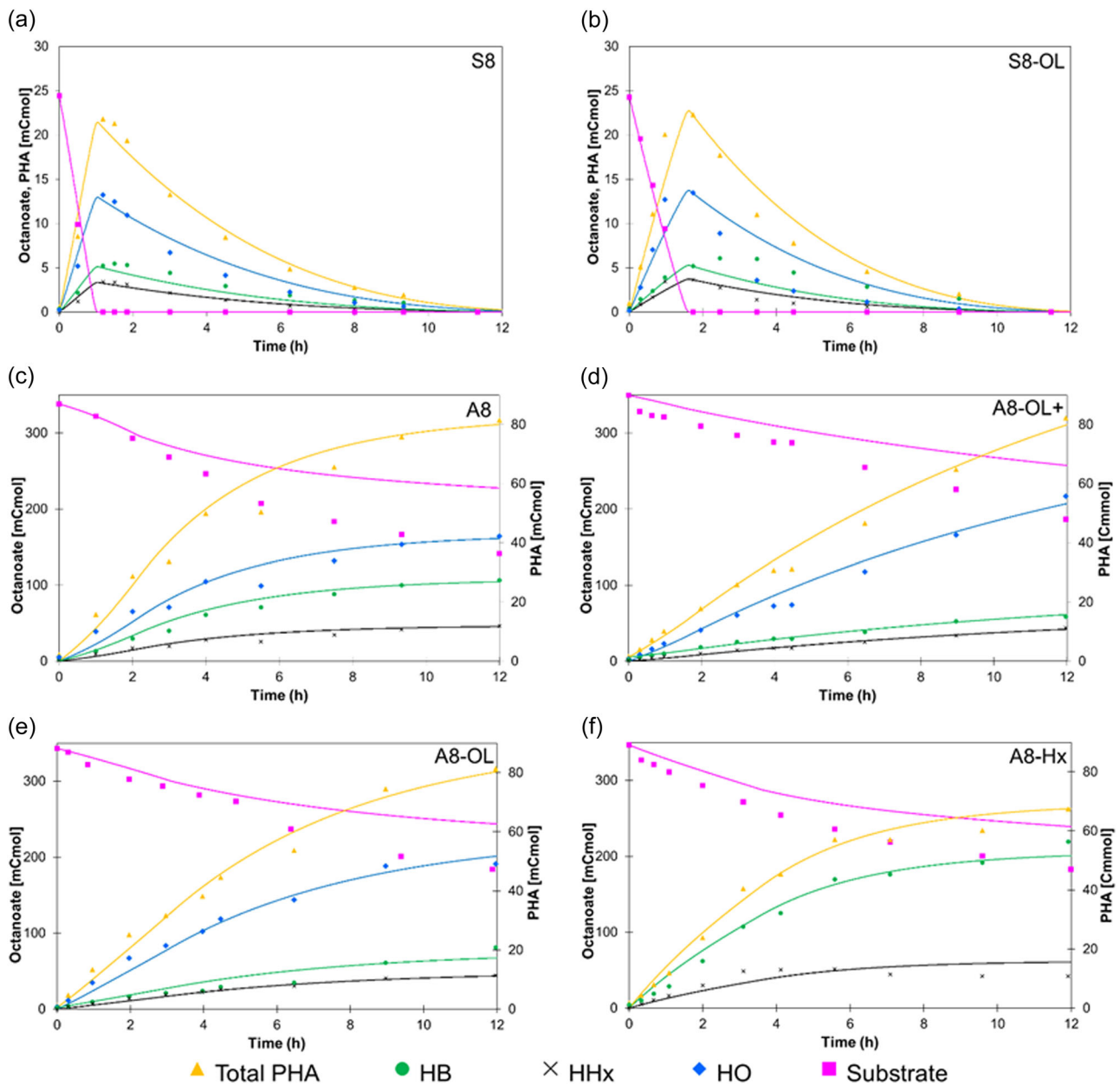


**FIGURE 5** Overview of PHA and substrate analysis of S8 (a), S8-OL (b), A8 (c), A8-OL+ (d), A8-OL (e), and A8-Hx (f). The symbols represent the measured data, while the lines represent the modeled data. The yellow data points represent the total amount of PHA in the bioreactor, which is a sum of the individual monomers (HO, HHx, HB). For the accumulations, the substrate consumption is presented as a cumulative curve starting and ending at an arbitrary value. In Supporting Information: Figure S2, all experimental results fitted with the metabolic model are shown, including off-gas, ammonium, and biomass. A8-OL, oxygen-limited accumulation; HB, hydroxybutyrate; HHx, hydroxyhexanoate; HO, hydroxyoctanoate; PHA, polyhydroxyalkanoate; S8-OL, SBR under oxygen limitation; SBR, sequencing batch reactors.

of 800 rpm at pH 8, a difference of 17%. This result makes it plausible that part of the octanoic acid did not dissolve in the above-described accumulation experiments as well.

TGA was used as a secondary PHA quantification method to validate the PHA analysis results of the GC (Chan et al., 2017). On average, the TGA measured  $3.0 \pm 2.6$  wt% higher than the GC which confirms that the applied GC method is reliable for mcl-PHA quantification (Table 1).

### 3.6 | Metagenomic analysis

One biomass sample, taken at the time of the cycle analysis of pH 7 (S7), was subjected to metagenomic analysis. The outcome revealed a relative abundance of 54% *Sphaerotilus natans*, which is in accordance with the 16S amplicon results. The remaining microbial community is very fractionated with the second most abundant microorganism only having a relative abundance of 0.6%.

The genome of *S. natans* displays the highest similarity with the subspecies *S. natans* subsp. *sulfidivorans* D-507 (accession: CP035708.1).

Two copies of the PHA synthase gene were found both in the genomic data of this study and in the online available genome of *S. natans* subsp. *sulfidivorans* D-507. The first synthase gene has 100% similarity with a PhaC class I synthase found in *S. natans* (McCool & Cannon, 2001). The second PHA synthase is classified as alpha/beta fold hydrolase in *S. natans* (Ollis et al., 1992), but it reveals a high similarity with PHA synthases in other microorganisms which are not assigned to a specific class of PHA synthases (e.g., 96% identities with PHA synthase in *Leptothrix* sp. C29) (Whitman et al., 2015). Although both PHA synthases have roughly the same size (~1200 nucleotides), the similarity between the two genes is low. Only two fragments of the genes revealed reasonable similarity. The first alignment had 154/271 (71%) identities, while the second alignment had 166/251 (66%) identities.

### 3.7 | Physicochemical properties

PHA from the accumulation experiments was purified from the biomass via a solvent extraction and subsequently analyzed for its physicochemical properties. The GPC chromatograms disclosed one PHA peak for each accumulation experiment with an average polydispersity index of  $2.4 \pm 0.4$ . The value of the molecular weight ( $M_w$ ) showed substantial variation between the experiments ranging from 263 to 1358 kDa. A trend was observed between the degree of polymerization and the monomer fraction of HB and HO in the polymer (Figure 6a). The degree of polymerization instead of  $M_w$  is

plotted in this figure to exclude the effect of the differently-sized monomers. A larger fraction of HB monomers and a smaller fraction of HO monomers correlate to a higher degree of polymerization. The HHx monomer fraction was fairly constant in all measurements regardless of the degree of polymerization.

To analyze if the PHA consists of a copolymer or different homopolymers, part of the extracted PHA of the accumulation at pH 8 (A8) was redissolved in chloroform and fractionated through precipitation with different volumes of 1-heptane. It appeared that the PHA can be effectively separated into an HB-rich fraction (91 wt% HB) and an HHx/HO-rich fraction (96 wt% HHx/HO) by adding 1.4 or more volumes of 1-heptane. Precipitation of the HHx/HO-rich fraction was not achieved, even after 15 volumes of 1-heptane and 48 h of incubation time at RT (Figure 6b). The  $M_w$  of the HB-rich fraction was 657 kDa (PDI = 3.0), while the  $M_w$  of the HHx/HO-rich fraction was 265 kDa (PDI = 1.7). This demonstrates that the PHA produced by the community in A8 with an average  $M_w$  of 497 kDa comprises a mixture of polymer chains differing both in size and monomeric composition rather than one copolymer.

The DSC curves revealed a high degree of similarity between all samples. Two melting temperature ( $T_m$ ) peaks were measured in each sample with an average value of  $143 \pm 6^\circ\text{C}$  and  $157 \pm 4^\circ\text{C}$ . A higher HB content seems to result in a slightly higher  $T_m$ , although the trend is not very distinct (Supporting Information: Figure S3). A8-Hx forms an exception: It does not follow this trend and has only one peak. A reference sample consisting mainly of HB monomers (94%) with a small fraction of hydroxyvalerate (HV) (2%) and HHx (4%) monomers also gave two melting peaks at slightly lower temperatures ( $137^\circ\text{C}$  and  $152^\circ\text{C}$ ).

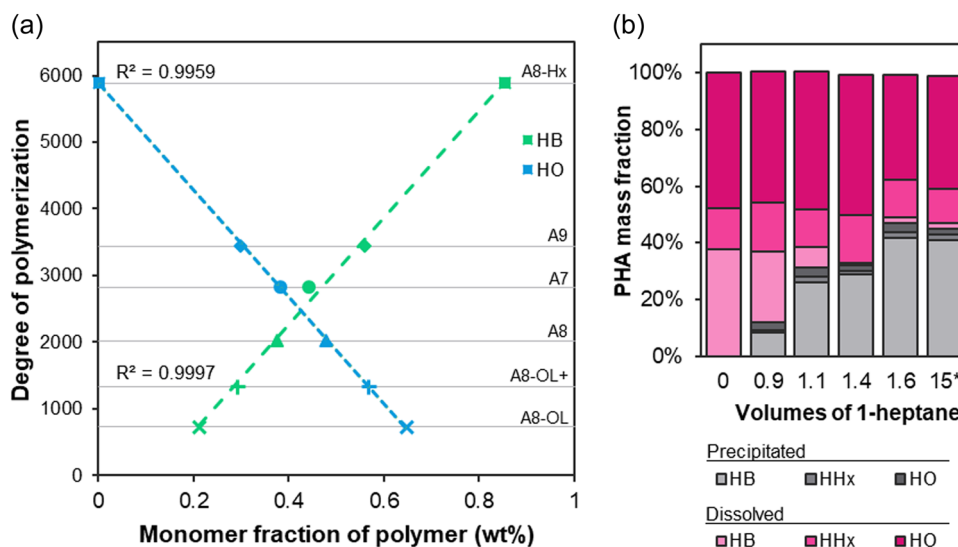


**FIGURE 6** Determination of polymer structure. (a) The degree of polymerization versus monomer composition for all accumulation experiments. A trendline was drawn through both the HB and HO data points. (b) PHA fractionation test. Different volumes of 1-heptane were added to chloroform with PHA dissolved from the accumulation at pH 8 at 12 h (S8). PHA was measured in both the pellet (precipitated) and supernatant (dissolved). \*The tubes with 15 volumes were incubated for 48 h instead of 15 min. A8-OL, oxygen-limited accumulation; HB, hydroxybutyrate; HHx, hydroxyhexanoate; HO, hydroxyoctanoate; PHA, polyhydroxyalkanoate.

## 4 | DISCUSSION

### 4.1 | Enrichment with a high PHA storage capacity

In this study, we demonstrated that enrichment cultures can be deployed for the selection of communities with a high mcl-PHA storage capacity. Accumulation under oxygen limitation resulted in a maximal PHA content of 76 wt%, where the mcl-PHA monomers were dominant (i.e., an HHx fraction of 0.14 and an HO fraction of 0.65). This is considerably higher than the 34 wt% reported in previous research investigating octanoate-fed enrichments, although the mcl-PHA fraction was similar (i.e., HHx fraction of 0.08 and HO fraction of 0.62) (Chen et al., 2018). Li et al. (2021) also obtained a lower PHA content (53 wt%) when enriching with octanoate as a cosubstrate, which also resulted in a significantly lower mcl-PHA fraction (i.e., HHx fraction of 0.08 and HO fraction of 0.26).

In scl-PHA studies, it was established that minimizing the number of SBR cycles per SRT is a crucial factor for the enrichment of communities with high PHA productivity. The reason is that the substrate-to-biomass ratio is increased leading to a higher PHA content at the end of the feast phase provided that substrate is predominantly used for PHA production (Jiang et al., 2011). In this study, the number of SBR cycles per SRT was deliberately set at a low value of 2 which is lower than the value extracted from other mcl-PHA studies whenever data were available (Table 2). Therefore, we argue that the low number of SBR cycles per SRT in this study was key for the high final PHA content compared to other studies where mcl-PHA is produced with enrichments.

### 4.2 | Mcl-PHA production as a selective strategy

Analysis of the pathways for octanoate metabolism revealed that an active beta-oxidation pathway is accompanied by the production of reduced electron carriers such as NADH (and  $FADH_2$ ) (R3-5 in Supporting Information: Figure S1). For PHB production, more cycles of the beta-oxidation are required and, therefore, more NADH is produced than for PHHx and PHO production. The production of biomass from octanoate also results in a net NADH production. NADH can be regenerated via oxidative phosphorylation resulting in the production of ATP (R12 in Supporting Information: Figure S1). When the degree of reduction of the substrate is high compared to

the storage polymer, oxidative regeneration of NADH is coupled to more ATP production than is actually needed in storage polymer production. Alternatively, ATP can be used in the maintenance reactions of the bacteria. However, under feast-famine conditions, the biomass-specific PHA production rates are relatively high compared to the biomass-specific maintenance reaction rates when the substrate is present (Table 1 and Supporting Information: - Figure S4). Therefore, maintenance reactions offer a relatively small sink for the surplus of ATP.

In Figure 7, the modeled surplus of ATP is shown for a hypothetical community that produces 100% PHB but with the kinetic parameters found in the enrichment at pH 8 (S8). The ATP surplus is positive in the feast phase, while it becomes negative in the famine. In reality, the bacteria have possibly several adaptations to eliminate a surplus of ATP such as lowering the substrate uptake rate, the dissipation of energy in futile cycles, increasing ATP requirements for maintenance, and decreasing the efficiency of the oxidative phosphorylation. However, the implementation of those adaptations will reduce the competitiveness of the community in the SBR.

When solely PHO is produced hypothetically, a shortage of ATP instead of a surplus can be reached in the feast phase, as can be seen

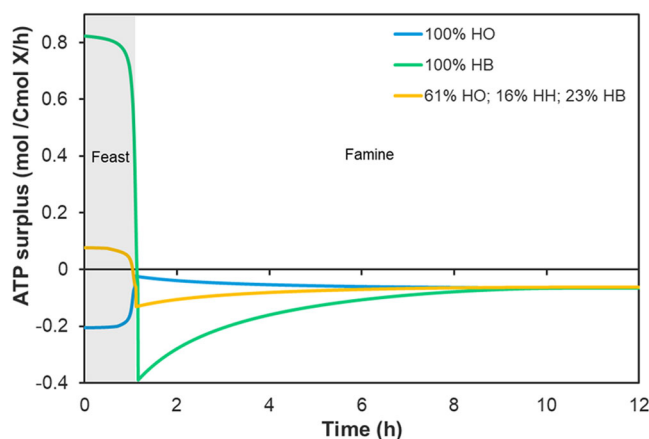


**FIGURE 7** Modeled ATP surplus (in mol ATP/Cmol X/h) for two hypothetical scenarios (blue and green line), and for SBR cycle at pH 8 (S8) (yellow line). The kinetic parameters ( $q_{s,max}$ ,  $\mu_{max}$ ,  $q_{PHA,max}$ ,  $m_{ATP}$ ,  $k_d$ ) were copied from the S8. HB, hydroxybutyrate; HO, hydroxyoctanoate; PHA, polyhydroxyalkanoate; SBR, sequencing batch reactor.

**TABLE 2** Number of SBR cycles per SRT and PHA content for studies enriching with medium-chain-length fatty acids

Study	Substrate	Number of cycles per SRT	PHA content after accumulation (wt%)
Lee et al. (2011)	Nonanoate	5.2	34
Chen et al. (2018)	Octanoate	3	49
This study	Octanoate	2	76

Note: Other studies do not display a value for the SRT.

Abbreviations: PHA, polyhydroxyalkanoate; SBR, sequencing batch reactor; SRT, solids retention time.

by the blue line in Figure 7. This shortage of ATP can be replenished by the complete oxidation of substrate via the tricarboxylic acid cycle. A third scenario is the production of a mixture of PHO, PHHx, and PHB as has been found in the experimental results of this study (S8). In this scenario indicated by the yellow line in Figure 7, the ATP surplus is minimal compared to the 100% PHB scenario. Overall, it appears that the scenario with mcl-PHA production does not result in a large energy surplus. Therefore, this theory suggests that mixed PHO, PHHx, and PHB production may be the direct result of the electron distribution between energy-consuming product formation pathways and respiration-driven energy production.

### 4.3 | Oxygen limitation as a tool to enhance mcl production

In aerobic feast–famine SBRs, the oxygen uptake rate profile during the cycle is a key indicator of the functional performance of the microbial community. When the community predominantly converted the substrate directly into biomass, the majority of the oxygen (~80%) was consumed in the feast phase (Figure 2b). A smaller fraction (~60%) of the oxygen was consumed in the feast phase when an scl-PHA production strategy was adopted by the community. The reason is that the produced PHA was oxidized in the famine phase to support growth. As explained in the previous section, mcl-PHA production in the feast phase results in a smaller surplus of ATP than scl-PHA production. Therefore, oxidative phosphorylation can be operated at a lower rate, thereby consuming less oxygen. This was confirmed in the first enrichment where an even smaller fraction (~30%) of the oxygen was consumed in the feast phase when mcl-PHA was produced. First, this makes oxygen consumption an important process performance indicator. Second, limiting oxygen supply becomes a potential selective tool to increase the mcl-PHA fraction. Although this tool has been successfully employed for enhancing mcl-PHA production in pure cultures (Blunt et al., 2017; Fernández et al., 2005) and for enhancing PHA yields in scl-PHA producing enrichments (Pratt et al., 2012; Third et al., 2003), it has never been demonstrated as a selective strategy to enhance mcl-PHA production in microbial enrichments. This study demonstrated that the mcl-fraction of the maximal PHA content increased from 0.62 to 0.79 when oxygen limitation was applied. Interestingly, another advantage of oxygen limitation is a 20% decrease in the PHA yield on oxygen ( $Y_{\text{PHA},\text{O}_2}$ ) under oxygen limitation compared to no oxygen limitation (Table 1). This indicates that less substrate is oxidized to reach the same quantity of PHA. It is difficult to determine this directly from the substrate uptake curve due to the unusually large gap in the mass balance.

### 4.4 | *Sphaerotilus* sp. as mcl-PHA producer

Microscopic observations, 16S amplicon, and metagenomic sequencing established that *Sphaerotilus natans* subsp. *sulfidivorans* were

dominant in all enrichments except at pH 9. Although *Sphaerotilus* sp. has been linked to PHB production (Takeda et al., 1995), this is, to our knowledge, the first report that links this genus to mcl-PHA production. Furthermore, *Sphaerotilus natans* is known to grow relatively well under conditions of low oxygen concentration (Pellegrin et al., 1999), which could explain why this species was also dominant in the oxygen-limited SBR (S8-OL). In a recent study by Grabovich et al. (2021), a comparative genome analysis was conducted on *S. natans* subsp. *sulfidivorans* and *S. natans* subsp. *natans*. It was proposed that the two bacteria should be reclassified as separate species, *S. sulfidivorans* sp. nov. and *S. natans*, based on a significant difference in genome characteristics and metabolic versatility.

### 4.5 | Polymer structure and microbial origin

The PHA fractionation experiment revealed that the enrichments in this study produced at least an HB-rich polymer, which could be effectively separated from the mcl-PHA fraction. For this reason, the polymer properties of the produced PHA are likely to be highly customizable. A study by Furrer et al. (2007) showed that poly(3-hydroxyhexanoate-co-octanoate) (PHHxO) can solubilize reasonably well in 1-hexane, which presumably also explains why the HHx/HO-rich fraction did not precipitate when 15 volumes of 1-heptane were added in this study.

The DSC data also suggests the presence of an HB-rich polymer, because a high melting temperature was found similar to the PHBVHx reference. From the literature, it is known that mcl-PHA exists predominantly in an amorphous state (Cai & Qiu, 2009; Fernández et al., 2005; Ruiz et al., 2019). Therefore, no clear melt transition exists when heat is applied, which could explain why no independent melting peaks appear on the DSC spectrum corresponding to the mcl-PHA. The low PDI of 1.7 of the HHx/HO-rich fraction suggests that the HHx and HO monomers are embedded in one copolymer.

In the genome of *S. sulfidivorans* sp. nov., two PhaC genes were found with significant differences. Alvarez-Santullano et al. (2021) state that members of the order *Burkholderia*, which is the order where *Sphaerotilus* sp. belongs, generally possess two or more different copies of the PhaC gene. It was also proposed that PhaC classification is more diverse than was previously known with the existence of additional classes. For *S. sulfidivorans* sp. nov., it is possible that one PhaC gene encodes for a PHA synthase that produces mainly PHB, while the other encodes for a PHA synthase that produces mainly PHHxO resulting in two different polymers instead of one copolymer in one microorganism. Both synthases will presumably have different characteristics, which may contribute to explaining the relation between the monomer content and the degree of polymerization (Figure 6a). Different physiological conditions result in differences in the activity of the two PHA synthases and subsequently different values of the overall  $M_w$ . Nevertheless, it is also possible that a second microbial species is responsible for part of the produced PHA.

## 4.6 | Outlook

To date, octanoate is present in most chain elongation studies and processes as a minor component (Holtzapfle et al., 2022). However, in recent years, the octanoate yield in these studies increased (Kucek et al., 2016), and it is expected that this trend will continue. Therefore, it is believed that octanoate valorization routes such as those described in this study will become more relevant in the future. Alternatively, the findings from this study (e.g., a low number of cycles per SRT or oxygen limitation) can possibly be extrapolated toward platform chemicals that are currently omnipresent in waste valorization routes such as hexanoate (Chen et al., 2017).

The bacterial species that were enriched at pH 7 and 8 (*S. sulfidivorans* sp. nov.) and at pH 9 (*Thauera* sp. or *Phreatobacter* sp.) were not yet linked to mcl-PHA production. This illustrates that large parts of the mcl-PHA biodiversity are still unexplored, and that microbial enrichments can be a powerful tool to explore these parts and to seek novel industrially relevant strains.

### AUTHOR CONTRIBUTIONS

**Chris M. Vermeer:** Investigation, conceptualization, verification, methodology, and writing – original draft. **Lena Depaz:** Conceptualization, verification, and investigation. **Emily van den Berg:** Methodology, verification, and investigation. **Tom Koelmans:** Verification and investigation. **Robbert Kleerebezem:** Funding acquisition, conceptualization, supervision, and writing – review and editing.

### ACKNOWLEDGMENTS

The authors would like to thank Stephen Picken for his advice on the polymer characterization results. This work was supported by the Netherlands Organization for Scientific Research (ALW/GK.2016.021). The authors also acknowledge the support of the companies Paques Biomaterials, Basilisk, and Cugla.

### DATA AVAILABILITY STATEMENT

The data that support the findings of this study are available from the corresponding author upon reasonable request.

### ORCID

Chris M. Vermeer  <http://orcid.org/0000-0002-1316-2012>

### REFERENCES

- Alaux, E., Couvreur, M., Marie, B., Bounouba, M., & Hernandez-Raquet, G. (2022). Biosynthesis of medium chain length polyhydroxyalkanoates (mcl-PHA) by activated sludge: Impact of phosphorus limitation on pha production and microbial diversity. *SSRN Electronic Journal*. Available at SSRN: <https://ssrn.com/abstract=4028808>.
- Altschul, S. F., Gish, W., Miller, W., Myers, E. W., & Lipman, D. J. (1990). Basic local alignment search tool. *Journal of Molecular Biology*, 215, 403–410.
- Alvarez-Santullano, N., Villegas, P., Mardones, M. S., Durán, R. E., Donoso, R., González, A., Sanhueza, C., Navia, R., Acevedo, F., Pérez-Pantoja, D., & Seeger, M. (2021). Genome-wide metabolic reconstruction of the synthesis of polyhydroxyalkanoates from sugars and fatty acids by *Burkholderia* Sensu Lato species. *Microorganisms*, 9, 1290.
- Angenent, L. T., Richter, H., Buckel, W., Spirito, C. M., Steinbusch, K. J. J., Plugge, C. M., Strik, D. P. B. T. B., Grootcholten, T. I. M., Buisman, C. J. N., & Hamelers, H. V. M. (2016). Chain elongation with reactor microbiomes: Open-culture biotechnology to produce biochemicals. *Environmental Science & Technology*, 50, 2796–2810.
- Anjum, A., Zuber, M., Zia, K. M., Noreen, A., Anjum, M. N., & Tabasum, S. (2016). Microbial production of polyhydroxyalkanoates (PHAs) and its copolymers: A review of recent advancements. *International Journal of Biological Macromolecules*, 89, 161–174.
- Beun, J. J., Dircks, K., Van Loosdrecht, M. C. M., & Heijnen, J. J. (2002). Poly- $\beta$ -hydroxybutyrate metabolism in dynamically fed mixed microbial cultures. *Water Research*, 36, 1167–1180.
- Blunt, W., Dartiaill, C., Sparling, R., Gapes, D., Levin, D. B., & Cicek, N. (2017). Microaerophilic environments improve the productivity of medium chain length polyhydroxyalkanoate biosynthesis from fatty acids in *Pseudomonas putida* LS46. *Process Biochemistry*, 59, 18–25.
- Cai, H., & Qiu, Z. (2009). Effect of comonomer content on the crystallization kinetics and morphology of biodegradable poly(3-hydroxybutyrate-co-3-hydroxyhexanoate). *Physical Chemistry Chemical Physics*, 11, 9569–9577.
- Chan, C. M., Johansson, P., Magnusson, P., Vandi, L. J., Arcos-Hernandez, M., Halley, P., Laycock, B., Pratt, S., & Werker, A. (2017). Mixed culture polyhydroxyalkanoate-rich biomass assessment and quality control using thermogravimetric measurement methods. *Polymer Degradation and Stability*, 144, 110–120.
- Chen, W. S., Strik, D. P. B. T. B., Buisman, C. J. N., & Kroeze, C. (2017). Production of caproic acid from mixed organic waste: An environmental life cycle perspective. *Environmental Science & Technology*, 51, 7159–7168.
- Chen, Z., Zhang, C., Shen, L., Li, H., Peng, Y., Wang, H., He, N., Li, Q., & Wang, Y. (2018). Synthesis of Short-Chain-Length and Medium-Chain-Length polyhydroxyalkanoate blends from activated sludge by manipulating octanoic acid and nonanoic acid as carbon sources. *Journal of Agricultural and Food Chemistry*, 66, 11043–11054.
- Elbahloul, Y., & Steinbüchel, A. (2009). Large-scale production of poly(3-hydroxyoctanoic acid) by *Pseudomonas putida* GPo1 and a simplified downstream process. *Applied and Environmental Microbiology*, 75, 643–651.
- Estévez-Alonso, Á., Pei, R., van Loosdrecht, M. C. M., Kleerebezem, R., & Werker, A. (2021). Scaling-up microbial community-based polyhydroxyalkanoate production: Status and challenges. *Bioresource Technology*, 327, 124790.
- Fernández, D., Rodríguez, E., Bassas, M., Viñas, M., Solanas, A. M., Llorens, J., Marqués, A. M., & Manresa, A. (2005). Agro-industrial oily wastes as substrates for PHA production by the new strain *Pseudomonas aeruginosa* NCIB 40045: Effect of culture conditions. *Biochemical Engineering Journal*, 26, 159–167.
- Fernández-Dacosta, C., Posada, J. A., Kleerebezem, R., Cuellar, M. C., & Ramirez, A. (2015). Microbial community-based polyhydroxyalkanoates (PHAs) production from wastewater: Techno-economic analysis and ex-ante environmental assessment. *Bioresource Technology*, 185, 368–377.
- Furrer, P., Panke, S., & Zinn, M. (2007). Efficient recovery of low endotoxin medium-chain-length poly([R]-3-hydroxyalkanoate) from bacterial biomass. *Journal of Microbiological Methods*, 69, 206–213.
- García-Ochoa, F., & Gomez, E. (2009). Bioreactor scale-up and oxygen transfer rate in microbial processes: An overview. *Biotechnology Advances*, 27, 153–176.
- Grabovich, M. Y., Smolyakov, D. D., Beletsky, A. V., Mardanov, A. V., Gureeva, M. V., Markov, N. D., Rudenko, T. S., & Ravin, N. V. (2021). Reclassification of *Sphaerotilus natans* subsp. *sulfidivorans* Gridneva et al. 2011 as *Sphaerotilus sulfidivorans* sp. nov. and comparative genome analysis of the genus *Sphaerotilus*. *Archives of Microbiology*, 203, 1595–1599.
- Holtzapfle, M. T., Wu, H., Weimer, P. J., Dalke, R., Granda, C. B., Mai, J., & Urgun-Demirtas, M. (2022). Microbial communities for valorizing

- biomass using the carboxylate platform to produce volatile fatty acids: A review. *Bioresource Technology*, 344, 126253.
- Jain, R., & Tiwari, A. (2015). Biosynthesis of planet friendly bioplastics using renewable carbon source. *Journal of Environmental Health Science and Engineering*, 13, 11.
- Jiang, Y., Marang, L., Kleerebezem, R., Muyzer, G., & van Loosdrecht, M. C. M. (2011). Effect of temperature and cycle length on microbial competition in PHB-producing sequencing batch reactor. *The ISME Journal*, 5, 896–907.
- Johnson, K., Jiang, Y., Kleerebezem, R., Muyzer, G., & van Loosdrecht, M. C. M. (2009). Enrichment of a mixed bacterial culture with a high polyhydroxyalkanoate storage capacity. *Biomacromolecules*, 10, 670–676.
- Johnson, K., Kleerebezem, R., & van Loosdrecht, M. C. M. (2009). Model-based data evaluation of polyhydroxybutyrate producing mixed microbial cultures in aerobic sequencing batch and fed-batch reactors. *Biotechnology and Bioengineering*, 104, 50–67.
- Kleerebezem, R., Joosse, B., Rozendal, R., & Van Loosdrecht, M. C. M. (2015). Anaerobic digestion without biogas? *Reviews in Environmental Science and Bio/Technology*, 14, 787–801.
- Kleerebezem, R., & van Loosdrecht, M. C. (2007). Mixed culture biotechnology for bioenergy production. *Current Opinion in Biotechnology*, 18, 207–212.
- Kourmentza, C., Plácido, J., Venetsaneas, N., Burniol-Figols, A., Varrone, C., Gavala, H. N., & Reis, M. A. M. (2017). Recent advances and challenges towards sustainable polyhydroxyalkanoate (PHA) production. *Bioengineering*, 4, 55.
- Kucek, L. A., Spirito, C. M., & Angenent, L. T. (2016). High n-caprylate productivities and specificities from dilute ethanol and acetate: Chain elongation with microbiomes to upgrade products from syngas fermentation. *Energy & Environmental Science*, 9, 3482–3494.
- Lee, S. H., Kim, J. H., Mishra, D., Ni, Y. Y., & Rhee, Y. H. (2011). Production of medium-chain-length polyhydroxyalkanoates by activated sludge enriched under periodic feeding with nonanoic acid. *Bioresource Technology*, 102, 6159–6166.
- Li, D., Ma, X., Yin, F., Qiu, Y., & Yan, X. (2021). Creating biotransformation of volatile fatty acids and octanoate as co-substrate to high yield medium-chain-length polyhydroxyalkanoate. *Bioresource Technology*, 331, 125031.
- Marang, L., van Loosdrecht, M. C. M., & Kleerebezem, R. (2016). Combining the enrichment and accumulation step in non-axenic PHA production: Cultivation of *Plasticicumulans acidivorans* at high volume exchange ratios. *Journal of Biotechnology*, 231, 260–267.
- McCool, G. J., & Cannon, M. C. (2001). PhaC and PhaR are required for polyhydroxyalkanoic acid synthase activity in *Bacillus megaterium*. *Journal of Bacteriology*, 183, 4235–4243.
- Ollis, D. L., Cheah, E., Cygler, M., Dijkstra, B., Frolow, F., Franken, S. M., Harel, M., Remington, S. J., Silman, I., Schrag, J., Sussman, J. L., Verschueren, K. H. G., & Goldman, A. (1992). The  $\alpha/\beta$  hydrolase fold. *Protein Engineering, Design and Selection*, 5, 197–211.
- Pabst, M., Grouzdev, D. S., Lawson, C. E., Kleikamp, H. B. C., de Ram, C., Louwen, R., Lin, Y. M., Lückner, S., van Loosdrecht, M. C. M., & Laurenzi, M. (2021). A general approach to explore prokaryotic protein glycosylation reveals the unique surface layer modulation of an anammox bacterium. *The ISME Journal: Multidisciplinary Journal of Microbial Ecology*, 2021 162 16, 346–357.
- Pellegrin, V., Juretschko, S., Wagner, M., & Cotteceau, G. (1999). Morphological and biochemical properties of a *Sphaerotilus* sp. isolated from paper mill slimes. *Applied and Environmental Microbiology*, 65, 156–162.
- Pereira, J. R., Araújo, D., Marques, A. C., Neves, L. A., Grandfils, C., Sevrin, C., Alves, V. D., Fortunato, E., Reis, M. A. M., & Freitas, F. (2019). Demonstration of the adhesive properties of the medium-chain-length polyhydroxyalkanoate produced by *Pseudomonas chlororaphis* subsp. *aurantiaca* from glycerol. *International Journal of Biological Macromolecules*, 122, 1144–1151.
- Pratt, S., Werker, A., Morgan-Sagastume, F., & Lant, P. (2012). Microaerophilic conditions support elevated mixed culture polyhydroxyalkanoate (PHA) yields, but result in decreased PHA production rates. *Water Science and Technology*, 65, 243–246.
- Quillaguamán, J., Guzmán, H., Van-Thuoc, D., & Hatti-Kaul, R. (2010). Synthesis and production of polyhydroxyalkanoates by halophiles: Current potential and future prospects. *Applied Microbiology and Biotechnology*, 85, 1687–1696.
- Rai, R., Keshavarz, T., Roether, J. A., Boccaccini, A. R., & Roy, I. (2011). Medium chain length polyhydroxyalkanoates, promising new biomedical materials for the future. *Materials Science & Engineering*, 72, 29–47.
- Ruiz, C., Kenny, S. T., Narancic, T., Babu, R., & Connor, K. O. (2019). Conversion of waste cooking oil into medium chain polyhydroxyalkanoates in a high cell density fermentation. *Journal of Biotechnology*, 306, 9–15.
- Shen, L., Hu, H., Ji, H., Zhang, C., He, N., Li, Q., & Wang, Y. (2015). Production of poly(3-hydroxybutyrate-co-3-hydroxyhexanoate) from excess activated sludge as a promising substitute of pure culture. *Bioresource Technology*, 189, 236–242.
- Silva, F., Matos, M., Pereira, B., Ralo, C., Pequito, D., Marques, N., Carvalho, G., & Reis, M. A. M. (2022). An integrated process for mixed culture production of 3-hydroxyhexanoate-rich polyhydroxyalkanoates from fruit waste. *Chemical Engineering Journal*, 427, 131908.
- Steinbüchel, A. (1991). Polyhydroxyalkanoic acids, *Biomaterials*. (pp. 123–213). Palgrave Macmillan.
- Steinbüchel, A., & Valentin, H. E. (1995). Diversity of bacterial polyhydroxyalkanoic acids. *FEMS Microbiology Letters*, 128, 219–228.
- Stouten, G. R. (2019). *Exploring microbial diversity extending the boundaries of biopolymer production using parallel cultivation* (PhD thesis). TU Delft University.
- Stouten, G. R., Hogendoorn, C., Douwenga, S., Kiliias, E. S., Muyzer, G., & Kleerebezem, R. (2019). Temperature as competitive strategy determining factor in pulse-fed aerobic bioreactors. *The ISME Journal*, 13, 3112–3125.
- Sudesh, K., Abe, H., & Doi, Y. (2000). Synthesis, structure and properties of polyhydroxyalkanoates: Biological polyesters. *Progress in Polymer Science*, 25, 1503–1555.
- Sun, Z., Ramsay, J. A., Guay, M., & Ramsay, B. A. (2007). Fermentation process development for the production of medium-chain-length poly-3-hydroxyalkanoates. *Applied Microbiology and Biotechnology*, 75, 475–485.
- Takeda, M., Matsuoka, H., Hamana, H., & Hikuma, M. (1995). Biosynthesis of poly-3-hydroxybutyrate by *Sphaerotilus natans*. *Applied Microbiology and Biotechnology*, 43, 31–34.
- Third, K. A., Newland, M., & Cord-Ruwisch, R. (2003). The effect of dissolved oxygen on PHB accumulation in activated sludge cultures. *Biotechnology and Bioengineering*, 82, 238–250.
- Tortajada, M., da Silva, L. F., & Prieto, M. A. (2013). Second-generation functionalized medium-chain-length polyhydroxyalkanoates: The gateway to high-value bioplastic applications. *International Microbiology*, 16, 1–15.
- Van't Riet, K. (1979). Review of measuring methods and results in nonviscous gas-liquid mass transfer in stirred vessels. *Industrial & Engineering Chemistry Process Design and Development*, 18, 357–364.
- Velasco Alvarez, M., ten Pierick, A., van Dam, P., Maleki Seifar, R., van Loosdrecht, M., & Wahl, S. (2017). Microscale quantitative analysis of polyhydroxybutyrate in prokaryotes using IDMS. *Metabolites*, 7, 19.
- Vermeer, C. M., Bons, L. J., & Kleerebezem, R. (2022). Production of a newly discovered PHA family member with an isobutyrate-fed enrichment culture. *Applied Microbiology and Biotechnology*, 106, 605–618.
- Vishniac, W., & Santer, M. (1957). The thiobacilli. *Bacteriological Reviews*, 21, 195–213.
- Whitman, W. B., Woyke, T., Klenk, H. P., Zhou, Y., Lilburn, T. G., Beck, B. J., De Vos, P., Vandamme, P., Eisen, J. A., Garrity, G., Hugenholtz, P., & Kyrpides, N. C. (2015). Genomic encyclopedia of bacterial and archaeal type strains, phase III: The genomes of soil and plant-associated and newly described type strains. *Standards in Genomic Sciences*, 10, 26.



Zheng, Y., Chen, J. C., Ma, Y. M., & Chen, G. Q. (2020). Engineering biosynthesis of polyhydroxyalkanoates (PHA) for diversity and cost reduction. *Metabolic Engineering*, 58, 82–93.

### SUPPORTING INFORMATION

Additional supporting information can be found online in the Supporting Information section at the end of this article.

**How to cite this article:** Vermeer, C. M., Depaz, L., den Berg, E., Koelmans, T., & Kleerebezem, R. (2022). Production of medium-chain-length PHA in octanoate-fed enrichments dominated by *Sphaerotilus* sp. *Biotechnology and Bioengineering*, 1–15. <https://doi.org/10.1002/bit.28306>